Theoretical treatment of the mixed ferro-ferrimagnets composed of ternary-metal Prussian blue analogs in a paramagnetic region

Shin-ichi Ohkoshi and Kazuhito Hashimoto*
Research Center for Advanced Science and Technology, The University of Tokyo, 4-6-1 Komaba, Meguro-ku, Tokyo 153-8904, Japan
(Received 16 April 1999; revised manuscript received 16 June 1999)

Our objective in the series of the present work is to obtain a type of magnet in which the weight average of ferromagnetic and ferrimagnetic characters is precisely controlled by fine tuning of the composition. For this attempt, we have prepared the $(Ni^{II}_xMn^{II}_{1-x})_{1.5}[Cr^{III}(CN)_6]\cdot zH_2O$ system, incorporating both ferromagnetic Ni^{II}-Cr^{III} (J_{NiCr}) and antiferromagnetic Mn^{II}-Cr^{III} (J_{MnCr}) exchange interactions. In this work, its magnetic properties in a *paramagnetic* region, such as magnetic susceptibility (χ) and Weiss temperature (θ_c), were studied. In general, the χ^{-1} value for typical ferromagnets and ferrimagnets should be zero at Curie temperature (T_c). However, the observed χ^{-1} value for $x=0.30$ of this system did not drop off at T_c. The theoretical analysis based on a molecular-field theory considering both ferromagnetic ($J_{NiCr}>0$) and antiferromagnetic ($J_{MnCr}<0$) exchange interactions showed that this phenomenon occurred because a compensation temperature is close to T_c. In addition, it showed that the variation of the θ_c value is not due to changes in the magnitudes of superexchange interactions but due to changes in the weighted average of J_{NiCr} and J_{MnCr} as a function of x. [S0163-1829(99)09941-5]

I. INTRODUCTION

Molecule-based magnetism has been studied actively for the last 10 years.[1–4] Up to date, various molecule-based magnets have been obtained with bimetallic,[5,6] metal-organic,[7,8] and organic systems.[9–11] The advantages of these type of magnets compared to classical-metal and metal-oxide ones are that the magnets can be obtained through a selection of proper spin sources (e.g., transition-metal ions, organic radicals) and coordinating ligands. Therefore, one of the goals in this field is the rational design of new magnets exhibiting novel magnetic properties. For the preparation of molecule-based magnets, the important issues can be summarized as follows: (1) What kinds of spin sources and ligands are chosen as building blocks? (2) How are the building blocks assembled, considering dimensionalities (one, two, or three dimensional) of their networks and the exchange interaction among their spin sources? From these points of view, Prussian blue, $Fe_4[Fe(CN)_6]_3\cdot zH_2O$, and its analogs are one of the most attractive classes of molecule-based magnets because various types of building blocks $[A(CN)_6]^{x-}$ and metal ions B can be assembled in an alternating fashion.[12–19]

The objective in the series of the present work is to design a new type of magnet, in which the weight average of ferromagnetic and ferrimagnetic characters is precisely controlled by fine tuning of the compositional factor. Here, we call this magnet a mixed ferro-ferrimagnet. For classical-metal or metal-oxide magnets, such an attempt is difficult in general. This is because various types of exchange and/or superexchange interactions (J) exist among metals or metal ions. Moreover, the metal substitution often causes structural distortions. Therefore, we have chosen Prussian blue analogs as target materials and recently prepared a series of $(Ni^{II}_xMn^{II}_{1-x})_{1.5}[Cr^{III}(CN)_6]$ compounds, which can accommodate both ferromagnetic and antiferromagnetic exchange interactions.[20,21] Their magnetic properties such as saturation magnetization (I_s) and compensation temperatures (T_{comp}) could be controlled by changing the compositional factor x. Moreover, these magnetic properties in a *ferromagnetic* region ($T<T_c$) could be analyzed well using a molecular field (MF) theory considering only two types of superexchange couplings between the nearest-neighbor sites.[21] This theoretical treatment showed that the mixed ferro-ferrimagnet composed of ternary Prussian blue analogs is one of the first systems to which we can apply the simple MF theory. In fact, in a mixed ferro-ferrimagnet $(Ni^{II}_aMn^{II}_bFe^{II}_c)_{1.5}[Cr^{III}(CN)_6]\cdot zH_2O$, we have recently succeeded in designing and synthesizing a novel type of magnet exhibiting two compensation temperatures, i.e., the spontaneous magnetization changes its sign twice with changing temperature.[22]

In this paper, we report the theoretical treatments of magnetic properties of the mixed ferro-ferrimagnet in *paramagnetic* region ($T\geqslant T_c$) using the $(Ni^{II}_xMn^{II}_{1-x})_{1.5}[Cr^{III}(CN)_6]$ system as a model compound, attempting to answer the following questions: (1) How does the temperature dependence of χ values change between a ferromagnet and a ferrimagnet? (2) What does the θ_c value of mixed ferro-ferrimagnets mean?

II. BACKGROUND

Let us first show the thermodynamics of magnetic susceptibility for typical ferromagnets and ferrimagnets as a background of this work. For ferromagnets, the magnetic susceptibility (χ) value above T_c obeys the Curie-Weiss law and hence the χ^{-1} value decreases linearly to zero at T_c.[23] For ferrimagnets, conversely, the χ^{-1} vs T curve deviates from the linear line and finally drops off to zero at T_c.[24] Moreover, the χT vs T plots are also useful for judging whether it is a ferromagnet or a ferrimagnet. For ferromagnets, the χT value increases monotonously, approaching infinity at T_c with decreasing temperature. Conversely, for ferrimagnets,

 ©1999 The American Physical Society

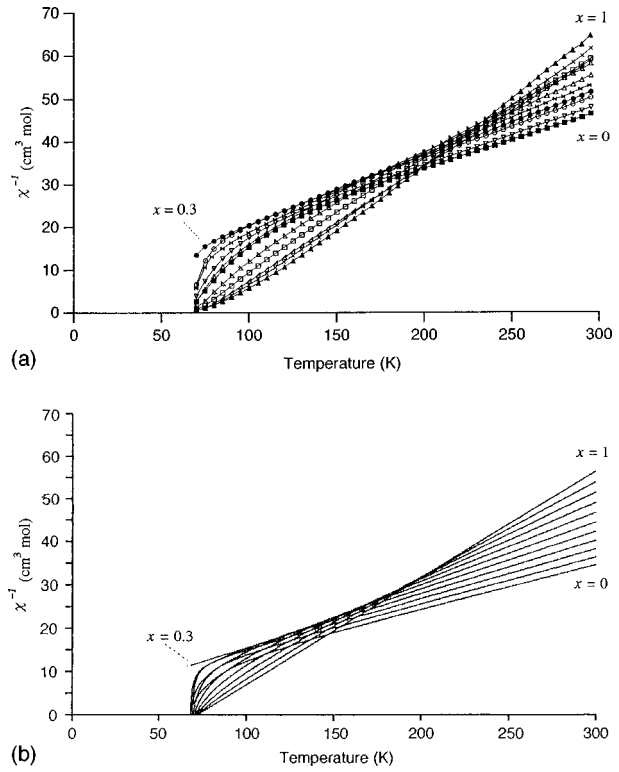

FIG. 1. (a) The experimental temperature dependence of the χ^{-1} curves for $(Ni^{II}_xMn^{II}_{1-x})_{1.5}[Cr^{III}(CN)_6]\cdot zH_2O$ [$x=0$(■), 0.11 (▽), 0.21 (○), 0.30 (●), 0.42 (⋈), 0.52 (△), 0.62 (◺), 0.71 (□), 0.81 (◿), 0.91 (×), 1 (▲)]. (b) The calculated temperature dependences of the χ^{-1} curves for $x=0,0.10,0.20,0.30,0.40,0.50,0.60,0.70,0.80,0.90,1$, going from the lowest curve to the highest curve at a high-temperature region based on the molecular-field theory, with three sublattice sites (Ni, Mn, Cr), with J coefficients $J_{NiCr}=5.6\,cm^{-1}$ and $J_{MnCr}=-2.5\,cm^{-1}$.

the χT vs T plots have a minimum value and then approach infinity at T_c. In addition, the sign of the Weiss temperature (θ_c) value is determined by the sign of superexchange interaction between spin sources, i.e., $\theta_c<0$ for an antiferromagnetic exchange, $\theta_c>0$ for a ferromagnetic exchange. Therefore, we can distinguish whether the magnet is a ferromagnet or a ferrimagnet by seeing its χ^{-1} vs T plots, χT vs T plots and the θ_c value. Note that observed χ^{-1} vs T plots for ferromagnets should be slightly shifted upward from the predicted line because the remaining clusters behave much as large paramagnetic molecules above T_c.[25]

III. MAGNETIC SUSCEPTIBILITY

In Fig. 1(a) the experimentally obtained χ^{-1} vs T plots in a series of $(Ni^{II}_xMn^{II}_{1-x})_{1.5}[Cr^{III}(CN)_6]$ are shown. At a high-temperature range ($T>150$ K), the slope of the χ^{-1} vs T plots increased with increasing x. This is reasonable because the χ^{-1} value for $Ni^{II}_{1.5}[Cr^{III}(CN)_6]\cdot 8H_2O$ ($S_{Ni}=1$, $S_{Cr}=\frac{3}{2}$) is larger than that for $Mn^{II}_{1.5}[Cr^{III}(CN)_6]\cdot 7.5H_2O$ ($S_{Mn}=\frac{5}{2}$, $S_{Cr}=\frac{3}{2}$). Concerning the curvature of χ^{-1} vs T plots around T_c, we had expected that a straight line would become a curved line monotonously with decreasing x. However, a complicated change was seen. For example, for $0.1\leqslant x\leqslant 0.5$, the curvatures were larger than that for $x=0$. Particularly, for $x=0.30$, the χ^{-1} vs T plots did not drop off near T_c. Similarly, in the χT vs T plots [Fig. 2(a)], the curve for $x=0.3$ showed anomalous temperature dependence: i.e., although the χT vs T curves for other compositions approached infinity at T_c, the curve for $x=0.3$ showed a straight line.

In order to understand these anomalous temperature dependences of the χ value, we carried out theoretical treatments of the χ values based on a MF theory. In the Prussian blue analogs, $A^{II}_y[B^{III}(CN)_6]$, the A^{II} and B^{III} metal ions are linked in an alternating fashion and hence the superexchange interaction between the second nearest-neighbor sites, A^{II}-A^{II} and B^{III}-B^{III}, can be neglected because of their long distances (~10 Å).[12–22] Therefore, in the MF model for $(Ni^{II}_xMn^{II}_{1-x})_{1.5}[Cr(CN)_6]$ system, only two types of superexchange couplings between the nearest-neighbor sites, one for ferromagnetic Ni^{II}-Cr^{III} and the other for antiferromagnetic Mn^{II}-Cr^{III} are considered. The molecular fields H_{Ni}, H_{Mn}, and H_{Cr} acting on the three sublattice sites can be expressed as follows:

$$H_{Mn}=n_{MnCr}M_{Cr}, \tag{1}$$

$$H_{Ni}=n_{NiCr}M_{Cr}, \tag{2}$$

$$H_{Cr}=n_{CrMn}M_{Mn}+n_{CrNi}M_{Ni}, \tag{3}$$

where various n_{ij} are the molecular-field coefficients, and M_{Ni}, M_{Mn}, and M_{Cr} are sublattice magnetizations per unit volume for the Ni, Mn, and Cr sites, respectively. On the basis of the Curie-Weiss law, sublattice magnetizations in a paramagnetic region can be expressed as follows:

$$M_{Mn}=\frac{C_{Mn}(H_0+H_{Mn})}{T}, \tag{4}$$

$$M_{Ni}=\frac{C_{Ni}(H_0+H_{Ni})}{T}, \tag{5}$$

$$M_{Cr}=\frac{C_{Cr}(H_0+H_{Cr})}{T}, \tag{6}$$

where H_0 is the external magnetic field, various C_i are Curie constants of each sublattice. The χ is defined as $\chi=(M_{Ni}+M_{Mn}+M_{Cr})/H_0$. Therefore, the χ^{-1} value can be evaluated using Curie constants and molecular-field coefficients as follows:

$$\chi^{-1}=-\frac{T^3-(C_{Ni}C_{Cr}n^2_{NiCr}+C_{Mn}C_{Cr}n^2_{MnCr})T}{(C_{Ni}+C_{Mn}+C_{Cr})T^2+(2C_{Ni}C_{Cr}n_{NiCr}+2C_{Mn}C_{Cr}n_{MnCr})T}+C_{Ni}C_{Mn}C_{Cr}(2n_{NiCr}n_{MnCr}-n^2_{MnCr}-n^2_{NiCr}). \tag{7}$$

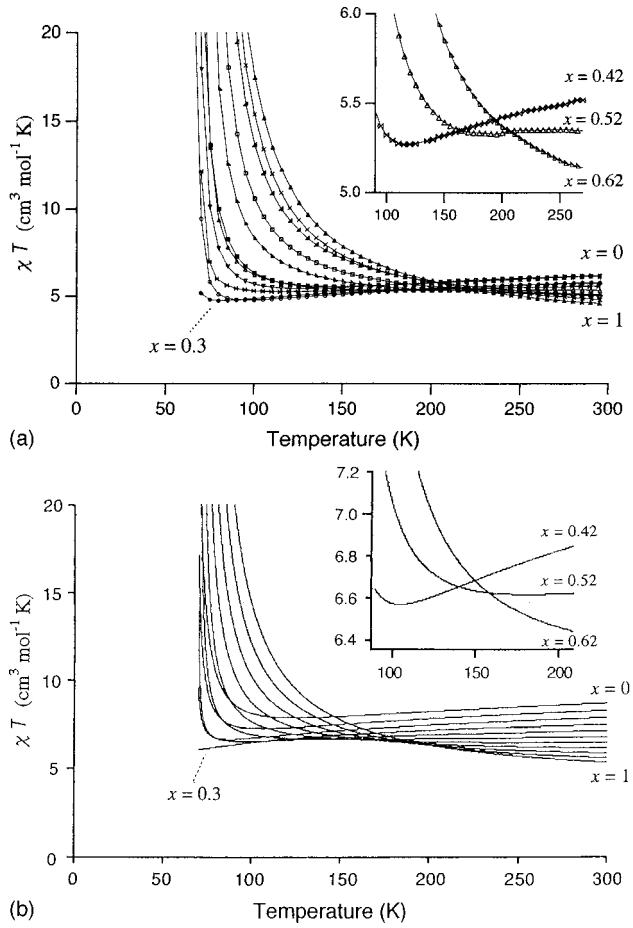

FIG. 2. (a) Experimental temperature dependences of the χT curves for $(Ni^{II}_{x}Mn^{II}_{1-x})_{1.5}[Cr^{III}(CN)_6]\cdot zH_2O$ [$x=0$(■), 0.11 (▽), 0.21 (○), 0.30 (●), 0.42 (⋈), 0.52 (△), 0.62 (◺), 0.71 (□), 0.81 (◿), 0.91 (×), 1 (▲)]. (b) Calculated temperature dependence of the $\chi^{-1}T$ curves for $x=0,0.10,0.20,0.30,0.40,0.50,0.60,0.70,0.80,0.90,1$, going from the highest curve to the lowest curve at a high-temperature region based on the molecular-field theory, with three sublattice sites (Ni, Mn, Cr), with J coefficients $J_{NiCr}=5.6\,cm^{-1}$ and $J_{MnCr}=-2.5\,cm^{-1}$.

The molecular-field coefficients n_{ij} are related to the exchange coefficients (J_{ij}) by

$$n_{MnCr}=\frac{2Z_{MnCr}}{\mu N(g\mu_B)^2}J_{MnCr}, \tag{8}$$

$$n_{NiCr}=\frac{2Z_{NiCr}}{\mu N(g\mu_B)^2}J_{NiCr}, \tag{9}$$

$$n_{CrMn}=\frac{2Z_{CrMn}}{\lambda_{Mn}N(g\mu_B)^2}J_{MnCr}, \tag{10}$$

$$n_{CrNi}=\frac{2Z_{CrNi}}{\lambda_{Ni}N(g\mu_B)^2}J_{NiCr}. \tag{11}$$

Conversely, Curie constants C_i are expressed as follows:

$$C_{Ni}=\frac{\lambda_{Ni}Ng^2\mu_B^2S_{Ni}(S_{Ni}+1)}{3k}, \tag{12}$$

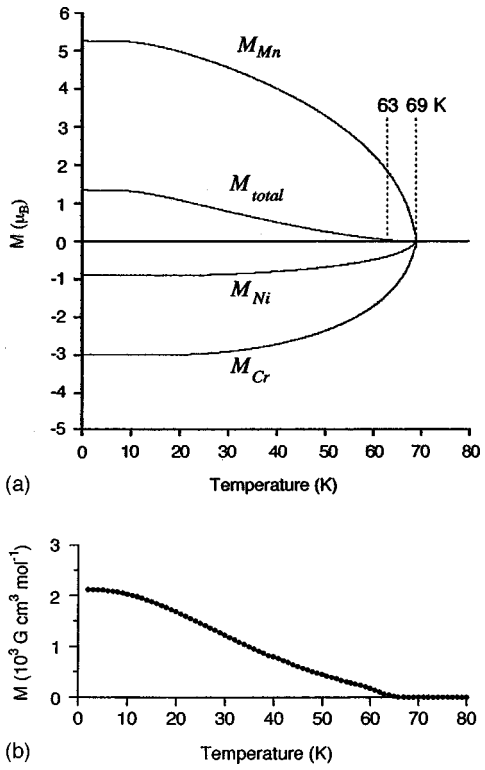

FIG. 3. (a) Calculated temperature dependence curves for each sublattice (M_{Mn}, M_{Ni}, M_{Cr}) and total magnetization (M_{total}) for $(Ni^{II}_{0.30}Mn^{II}_{0.70})_{1.5}[Cr^{III}(CN)_6]$ based on the three sublattice molecular-field theory, with J coefficients $J_{NiCr}=5.6\,cm^{-1}$ and $J_{MnCr}=-2.5\,cm^{-1}$. (b) Experimental magnetization vs temperature curves for $(Ni^{II}_{0.30}Mn^{II}_{0.70})_{1.5}[Cr^{III}(CN)_6]\cdot 7.5H_2O$ in the external field of 10 G.

$$C_{Mn}=\frac{\lambda_{Mn}Ng^2\mu_B^2S_{Mn}(S_{Mn}+1)}{3k}, \tag{13}$$

$$C_{Cr}=\frac{\mu Ng^2\mu_B^2S_{Cr}(S_{Cr}+1)}{3k}, \tag{14}$$

where μ_B is the Bohr magneton, Z_{ij} are the numbers of the nearest-neighbor j-site ions surrounding an i-site ion: $Z_{MnCr}=Z_{NiCr}=4$; $Z_{CrNi}=6x$; $Z_{CrMn}=6(1-x)$, N is the total number of all types of metal ions per unit volume, and λ_{Ni}, λ_{Mn}, and μ represent the mole fractions: $\lambda_{Ni}=1.5x$; $\lambda_{Mn}=1.5(1-x)$; $\mu=1$, respectively, and other quantities are as follows: $S_{Mn}=\frac{5}{2}$; $S_{Ni}=1$; $S_{Cr}=\frac{3}{2}$; and $g=2$. A J_{NiCr} value of $+5.6\,cm^{-1}$ and a J_{MnCr} value of $-2.5\,cm^{-1}$ were obtained from the experimental T_c values of $Ni^{II}_{1.5}[Cr^{III}(CN)_6]\cdot 8H_2O$ ($T_c=72$ K) and $Mn^{II}_{1.5}[Cr^{III}(CN)_6]\cdot 7.5H_2O$ ($T_c=67$ K), respectively.[21] Using these parameters, the temperature dependences of χ^{-1} values of $(Ni^{II}_{x}M^{III}_{1-x})_{1.5}[Cr^{III}(CN)_6]\cdot zH_2O$ system were calculated for several different compositions of x. As shown in Fig. 1(b), for $0.1\leqslant x\leqslant 0.5$, the curvatures near T_c were larger than that for $x=0$. Particularly, for $x=0.30$, the χ^{-1} vs T plots did not drop off near T_c. These calculated curves reproduced experimental curves qualitatively. In addition, the calculated $\chi T-T$ plots also reproduced the observed ones qualitatively as shown in Fig. 2(b).

Here, let us focus on the magnetic behavior for $x=0.30$, in order to understand its anomalous thermodynamics. Previously, we showed that the magnetization vs temperature curves below T_c exhibit various types of thermodynamics of magnetization depending on x.[20,21] Particularly, the compounds in which x was in the range of $0.38 \leqslant x \leqslant 0.42$ exhibited compensation temperatures (T_{comp}).[24,26–29] This occurred because the negative magnetization due to the Mn^{II} sublattice and the positive magnetizations due to the Ni^{II} and Cr^{III} sublattices have different temperature dependences. Calculated thermodynamics of magnetization for $x=0.30$ below T_c are shown in Fig. 3(a). Its total magnetization cannot appear in the region of $63\,K < T < 69\,K$, although the temperature is already lower than the theoretical $T_c(=69\,K)$ value evaluated by the following equation:

$$T_c = \sqrt{C_{Mn}C_{Cr}n_{MnCr}^2 + C_{Ni}C_{Cr}n_{NiCr}^2}. \tag{15}$$

The reason for this is that the sum of positive magnetizations of Ni^{II} and Cr^{III} sublattices is almost equivalent to the negative magnetization of Mn^{II}. In other words, for this composition, an antiferromagnetic behavior appears at near T_c. This means that T_{comp} is close to T_c. In fact, the observed magnetization vs temperature curve for $x=0.30$ showed a similar behavior as shown in Fig. 3(b). Usually, the χ^{-1} vs T plots for typical antiferromagnets show a straight line near T_c.

IV. WEISS TEMPERATURE

We finally discuss Weiss temperatures of the mixed ferro-ferrimagnet. The θ_c value is a significant parameter for mixed ferro-ferrimagnets because its sign is determined by the superexchange interaction between spin sources, i.e., $\theta_c < 0$ for an antiferromagnetic exchange, $\theta_c > 0$ for a ferromagnetic exchange. We carried out theoretical treatments of θ_c values using the MF model. Equation (7) is rewritten in the following form:

$$\chi^{-1} = \frac{T}{C_{Ni}+C_{Mn}+C_{Cr}} + \frac{1}{\chi_0} - \frac{\gamma T + \sigma}{T^2 - \alpha T + \beta}, \tag{16}$$

where the second term and the α, b, γ, and σ of the third terms on the right side are expressed by

$$\frac{1}{\chi_0} = -\frac{2C_{Ni}C_{Cr}n_{NiCr} + 2C_{Mn}C_{Cr}n_{MnCr}}{(C_{Ni}+C_{Mn}+C_{Cr})^2}, \tag{17}$$

$$\alpha = -\frac{2C_{Ni}C_{Cr}n_{NiCr} + 2C_{Mn}C_{Cr}n_{MnCr}}{C_{Ni}+C_{Mn}+C_{Cr}}, \tag{18}$$

$$\beta = -\frac{C_{Ni}C_{Mn}C_{Cr}(2n_{NiCr}n_{MnCr} - n_{MnCr}^2 - n_{NiCr}^2)}{C_{Ni}+C_{Mn}+C_{Cr}}, \tag{19}$$

$$\gamma = -\frac{2C_{Ni}C_{Cr}n_{NiCr} + 2C_{Mn}C_{Cr}n_{MnCr}}{C_{Ni}+C_{Mn}+C_{Cr}} + \frac{C_{Ni}C_{Mn}C_{Cr}(2n_{NiCr}n_{MnCr} - n_{MnCr}^2 - n_{NiCr}^2)}{(C_{Ni}+C_{Mn}+C_{Cr})^2} - \frac{(2C_{Ni}C_{Cr}n_{NiCr} + 2C_{Mn}C_{Cr}n_{MnCr})^2}{(C_{Ni}+C_{Mn}+C_{Cr})^3}, \tag{20}$$

$$\sigma = -\frac{C_{Ni}C_{Mn}C_{Cr}(2C_{Ni}C_{Cr}n_{NiCr} + 2C_{Mn}C_{Cr}n_{MnCr})(2n_{NiCr}n_{MnCr} - n_{MnCr}^2 - n_{NiCr}^2)}{(C_{Ni}+C_{Mn}+C_{Cr})^3}. \tag{21}$$

The first two terms on the right side of Eq. (16) represent the asymptotic line to which the χ^{-1}-T curve should approach at high temperature because the third term must vanish at $T \to \infty$. The extrapolation of this asymptote intersects the abscissa at the θ_c value. Therefore, the θ_c value is expressed by

$$\theta_c = \frac{2C_{Ni}C_{Cr}n_{NiCr} + 2C_{Mn}C_{Ci}n_{MnCr}}{C_{Ni}+C_{Mn}+C_{Cr}} = \frac{2S_{Cr}(S_{Cr}+1)[2\lambda_{Ni}S_{Ni}(S_{Ni}+1)Z_{NiCr}I_{NiCr} + 2\lambda_{Mn}S_{Mn}(S_{Mn}+1)Z_{MnCr}J_{MnCr}]}{3k[\lambda_{Ni}S_{Ni}(S_{Ni}+1) + \lambda_{Mn}S_{Mn}(S_{Mn}+1) + \mu S_{Cr}(S_{Cr}+1)]}. \tag{22}$$

This equation indicates that the variation of the θ_c value is due not to changes in the magnitudes of superexchange interactions (J_{NiCr}, J_{MnCr}), but to changes in the weighted average of J_{NiCr} and J_{MnCr} as a function of x. As shown in Fig. 4, the θ_c values were calculated for the whole x in the series of $(Ni^{II}_{x}Mn^{II}_{1-x})_{1.5}[Cr^{III}(CN)_6]\cdot zH_2O$. The θ_c values were expected to increased from negative to positive values showing a curved line.

The experimental θ_c values were plotted in Fig. 4 as circles. Those for $0 \leqslant x \leqslant 0.4$ corresponded to calculated values but those for $0.4 < x \leqslant 1$ were slightly off calculated values. In the present MF theory, we have not taken account of the spin cluster formation. As was described in Sec. II, the practical χ^{-1} vs T plots for ferromagnets are slightly shifted from the straight line due to the remaining spin clusters.[25] In fact, the observed χ^{-1} vs T plot for $x=1$ was slightly curved, resulting that its experimental θ_c value, which was obtained from the data fitting in the temperature range from 150 to 300 K, was larger than the calculated one. In this manner, the experimental θ_c values are slightly different from the θ_c values calculated by the MF model. These deviations are expected to be increased with increasing x because, for ferrimagnets, the asymptotic line of the χ^{-1} vs T plot in the present temperature range ($150\,K < T < 300\,K$) is not so influenced by spin clusters and hence the experimental θ_c value is close to the calculated ones. Therefore, the ex

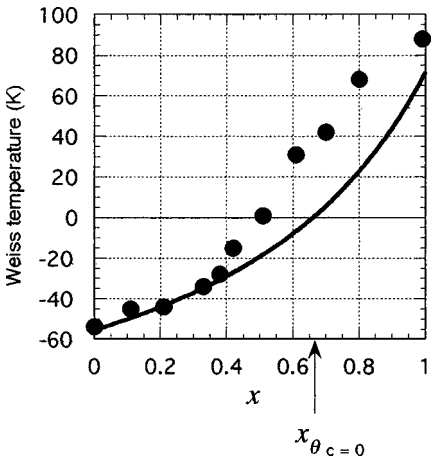

FIG. 4. Plots of θ_c values versus x: calculated curve(—) based on Eq. (22); observed (●). The θ_c values were extracted by the least-squares fitting of the data between room temperature and 150 K.

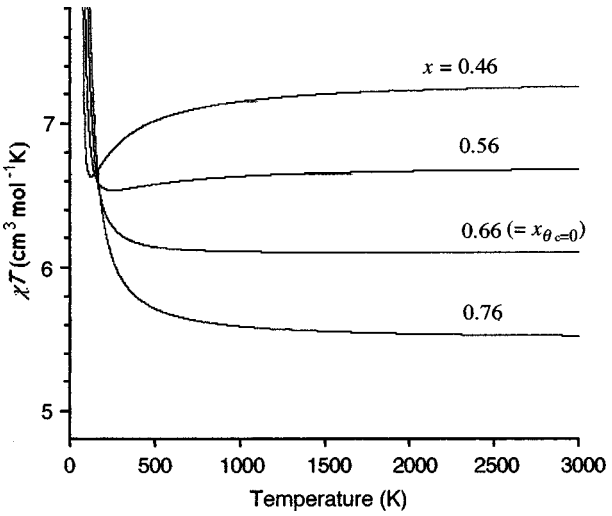

FIG. 5. Calculated temperature dependence of the $\chi^{-1}T$ curves in the region of $T_c < T < 3000$ K.

perimental θ_c values are becoming larger than the calculated ones gradually with increasing x.

Furthermore, we discuss the relationship between the sign of θ_c values and the shape of the $\chi T - T$ plots. The composition ($x_{\theta c=0}$) for the $\theta_c = 0$ is expressed as follows:

$$x_{\theta_c=0} = \left(1 - \frac{S_{\mathrm{Ni}}(S_{\mathrm{Ni}}+1)J_{\mathrm{NiCr}}}{S_{\mathrm{Mn}}(S_{\mathrm{Mn}}+1)J_{\mathrm{MnCr}}}\right)^{-1}. \tag{23}$$

When x is smaller than $x_{\theta c=0}$, θ_c is negative. Conversely, when x is larger than $x_{\theta c=0}$, θ_c is positive;

$$x < x_{\theta_c} = 0, \quad \theta_c < 0,$$

$$x \geqslant x_{\theta_c=0}, \quad \theta_c \geqslant 0. \tag{24}$$

The $x_{\theta c=0}$ of this system was calculated to be 0.66. This $x_{\theta c=0}$ value was different from either the composition of disappearance of saturation magnetization ($x = 0.429$) as described in our previous paper[22] or the composition of the anomalous χ^{-1} vs T plots ($x = 0.30$). In χT vs T plots of $T_c < T < 300$ K [Figs. 2(a) and 2(b)], the composition for $x = 0.52$ seems to be the threshold where the minimum value can appear. However, it is not the real threshold. In Fig. 5 calculated $\chi T - T$ plots of $T_c < T < 3000$ K are shown. These plots show that the real threshold for the appearance of minimum χT is $x = 0.66$ ($= x_{\theta c=0}$). Therefore, we can conclude that the $x_{\theta c=0}$ value corresponds the threshold where the minimum value can appear in χT vs T plots. Note that experimental measurement of this value is impossible because prepared samples decompose above 373 K.

V. CONCLUSION

We have succeeded in analyzing magnetic properties of mixed ferro-ferrimagnets in a paramagnetic region using the MF theory considering both ferromagnetic ($J_{\mathrm{NiCr}} > 0$) and antiferromagnetic ($J_{\mathrm{MnCr}} < 0$) exchange interactions. Particularly, the complicated change of the χ^{-1} vs T plots and the χT vs T plots were reproduced well. These complicated changes arise for the magnets with which T_{comp} values are close to T_c values. In addition, the θ_c values were suggested to increase from negative to positive values showing a curved line as a function of x. For the present system, the MF model reproduced the observed data qualitatively. The reasons for this success are as follows: (1) The fcc structure of the Prussian-blue analogs is maintained even when metal-ion substitution is carried out. (2) The superexchange interactions between the second nearest-neighbor sites can be neglected because of their long distances. (3) The divalent metal ions (Ni^{II} and Mn^{II}) and the trivalent metal ion (Cr^{III}) of the present materials are linked in an alternating fashion. By the combination of the above reasons, the ferromagnetic ($J > 0$) and antiferromagnetic ($J < 0$) exchange interactions can coexist without a spin-glass behavior. The mixed ferro-ferrimagnet composed of a ternary-metal Prussian blue analog is one of the first systems to which we can apply the simple MF theory and can predict magnetic properties. In fact, we have already succeeded in demonstrating a photoinduced magnetic pole inversion with the $(Fe^{II}_x Mn^{II}_{1-x})_{1.5}[Cr^{III}(CN)_6]\cdot 7.5H_2O$ based on the theoretical prediction using the MF theory.[30] In addition, we have recently succeeded in designing and synthesizing a type of magnet exhibiting two compensation temperatures with the $(Ni^{II}_a Mn^{II}_b Fe^{II}_c)_{1.5}[Cr^{III}(CN)_6]\cdot zH_2O$ system.[22] We thus believe that various novel magnets can be designed with Prussian blue analogs based on the MF theory.[31]

ACKNOWLEDGMENT

This work was supported by a Grant-in-Aid for Scientific Research on priority areas of electrochemisty of ordered interfaces from the Ministry of Education, Science, and Culture of Japan.

*Author to whom correspondence should be addressed.
[1] O. Kahn, *Molecular Magnetism* (VCH, New York, 1993).
[2] D. Gatteschi*et al.*, O. Kahn, J. S. Miller, and F. Palacio, *Magnetic Molecular Materials* (Kluwer, Dordrecht, Netherlands, 1991).
[3] J. S. Miller and A. J. Epstein, Angew. Chem. Int. Ed. Engl. **33**, 385 (1994).
[4] F. Palacio, G. Antorrena, M. Castro, R. Burriel, J. Rawson, and J. N. B. Smith, Phys. Rev. Lett. **79**, 2336 (1997).
[5] O. Kahn, Y. Pei, M. Verdaguer, J. P. Renard, and J. Sletten, J. Am. Chem. Soc. **110**, 782 (1988).
[6] H. Tamaki, Z. J. Zhong, N. Matsumoto, S. Kida, M. Koikawa, N. Achiva, Y. Hashimoto, and H. Okawa, J. Am. Chem. Soc. **114**, 6974 (1992).
[7] J. S. Miller, J. C. Calabrese, H. Rommelmmann, S. R. Chittipeddi, J. H. Zhang, W. M. Reiff, and A. J. Epstein, J. Am. Chem. Soc. **109**, 769 (1987).
[8] J. M. Manriquenz, G. T. Yee, R. S. McLean, A. J. Epstein, and J. S. Miller, Science **252**, 1415 (1991).
[9] K. Awaga and Y. Maruyama, J. Phys. Chem. **91**, 2743 (1989).
[10] M. Tamura, Y. Nakazawa, D. Shiomi, K. Nozawa, Y. Hosokoshi, M. Ishikawa, M. Takahashi, and M. Kinoshita, Chem. Phys. Lett. **186**, 401 (1991).
[11] P. M. Allemand, K. C. Khemani, A. Koch, F. Wudl, K. Holczer, S. Donovan, G. Grüner, and J. D. Thompson, Science **253**, 301 (1991).
[12] A. N. Hoden, B. T. Matthias, P. W. Anderson, and H. W. Luis, Proc. R. Soc. Med. **102**, 1463 (1956).
[13] W. D. Griebler and D. Babel, Z. Naturforsch. B **87**, 832 (1982).
[14] T. Mallah, S. Thiebaut, M. Verdaguer, and P. Veillet, Science **262**, 1554 (1993).
[15] W. R. Entley and G. S. Girolami, Inorg. Chem. **33**, 5165 (1994).
[16] S. Ferlay, T. Mallah, R. Ouahés, P. Veillet, and M. Verdaguer, Nature (London) **378**, 701 (1995).
[17] R. E. William and G. S. Girolami, Science **268**, 397 (1995).
[18] O. Sato, T. Iyoda, A. Fujishima, and K. Hashimoto, Science **271**, 49 (1996).
[19] M. Verdaguer, T. Mallah, V. Gadet, I. Castro, C. Hélary, S. Thiébaut, and P. Veillet, Conf. Coord. Chem. **14**, 19 (1993).
[20] S. Ohkoshi, O. Sato, T. Iyoda, A. Fujishima, and K. Hashimoto, Inorg. Chem. **36**, 268 (1997).
[21] S. Ohkoshi, T. Iyoda, A. Fujishima, and K. Hashimoto, Phys. Rev. B **56**, 11 642 (1997).
[22] S. Ohkoshi, Y. Abe, A. Fujishima, and K. Hashimoto, Phys. Rev. Lett. **82**, 1285 (1999).
[23] P. Weiss, J. de Physique **6**, 661 (1907).
[24] L. Néel, Ann. Phys. (Leipzig) **3**, 137 (1948).
[25] S. Chikazumi, *Physics of Magnetism* (Wiley, New York, 1964), p. 357.
[26] E. W. Gorter, Philips Res. Rep. **9**, 295 (1954); **9**, 321 (1954); **9**, 403 (1954).
[27] B. Lüthi, Phys. Rev. **148**, 519 (1966).
[28] C. Mathoniére, C. J. Nuttal, S. G. Carling, and P. Day, Inorg. Chem. **35**, 1201 (1996).
[29] S. A. Chavan, R. Granguly, V. K. Jain, and J. V. Yakhmi, J. Appl. Phys. **79**, 5260 (1996).
[30] S. Ohkoshi, S. Yorozu, O. Sato, T. Iyoda, A. Fujishima, and K. Hashimoto, Appl. Phys. Lett. **70**, 1040 (1997).
[31] S. Ohkoshi, A. Fujishima, and K. Hashimoto, J. Am. Chem. Soc. **120**, 5349 (1998).